Interplay between climate change and climate variability: the 2022 drought in Central South America

Paola A. Arias · Juan Antonio Rivera · Anna A. Sörensson″ · Mariam Zachariah · Clair Barnes · Sjoukje Philip, et al. *[full author details at the end of the article]*

Abstract

Since 2019, Central South America (CSA) has been reeling under drought conditions, with the last 4 months of 2022 receiving only 44% of the average total precipitation. Simultaneously to the drought, a series of record-breaking heat waves has affected the region. The rainfall deficit during October–November-December (OND) is highly correlated with the Niño3.4 index, indicating that the OND 2022 rainfall deficit is partly driven by La Niña, as observed in previous droughts in this region. To identify whether human-induced climate change was also a driver of the OND 2022 rainfall deficit, we analysed precipitation over the most impacted region. Our findings revealed a pattern of decreased rainfall over the past 40 years, although we cannot definitively conclude whether this trend exceeds what would be expected from natural variations. To clarify if this trend can be attributed to climate change, we looked at 1-in-20-year low rainfall events over the same region in climate models. The models show that the severity of low rainfall events decreases (i.e. they become wetter, the opposite of the trend observed in most weather records), although this trend is again not significant and is compatible with natural variability. Therefore, we cannot attribute the low rainfall to climate change. Moreover, our analysis of effective precipitation potential (evapotranspiration minus rainfall) shows that, in climate models, the increase in temperature does partly compensate for the increase in rainfall but only to offset the wetting, and does not lead to a significant climate change signal in effective precipitation. However, higher temperatures in the region, which have been attributed to climate change, decreased water availability in the models in late 2022, indicating that climate change probably reduced water availability over this period also in the observations, increasing agricultural drought, although this study did not quantify this effect. This means that even though the reduced rainfall is within the natural variability, the consequences of drought are becoming more severe due to the strong increase in extreme heat. The case of the OND 2022 rainfall deficit and the ongoing drought in CSA is a clear example of the interplay between climate variability and human-induced climate change. This shows the importance of considering not only those aspects associated with climate change but also climate variability in order to understand and attribute particular events or trends at the regional level.

1 Introduction

Droughts are among the most impactful extremes of the water cycle. The Sixth Assessment Report of the Intergovernmental Panel on Climate Change reports that droughts are increasing in frequency and intensity over many regions worldwide (IPCC 2021; Seneviratne et al. 2021). Moreover, the concurrent occurrence of droughts and heat extremes increases the water-related risks around the world (Caretta et al. 2022), for instance, in South America (Castellanos et al. 2022).

During the last six decades, Central South America (CSA) has experienced several prolonged and intense droughts, with widespread impacts on the agricultural and hydrological sectors and, therefore, on the regional economy and society. The drought events that affected a large portion of this region occurred mainly during the decade of 1960 and the first half of the 1970s, but also during the years 1988–1989, 1995–1996, 2006, 2008–2009, 2011, 2017–2018 and 2019–2023 (Rivera and Penalba 2014; Naumann et al. 2019, 2023). The 1988–1989 drought had significant impacts on the economic sector of Argentina and Uruguay, with severe agricultural production losses, high mortality of animals and minimum levels of hydroelectric power generation (Rivera and Penalba 2014; Cruz et al. 2018). During the 2008–2009 event, more than half of the total population of Argentina and almost 30% of the agricultural land were affected (Naumann et al. 2019). The severity of the 2008–2009 drought was the highest recorded since 1935, when the 'Pampas Dust Bowl' took place (Tripaldi et al. 2013). The direct agricultural losses reached about 3% of the GDP of Uruguay, although the estimated total losses (direct and indirect) for the Uruguayan economy tripled that value (Cruz et al. 2018). Direct production losses for maize and soybean in Argentina during the 2017–2018 flash drought episode were estimated at US\$ 1550 million, with an overall impact of about US\$ 4600 million to the Argentine economy (Bert et al. 2021). In Uruguay, the estimated national loss due to lower soybean yields during this drought event was slightly more than US\$ 445 million (Hernández et al. 2018).

Most of the historical drought events over CSA are linked to the El Niño-Southern Oscillation (ENSO), in particular to the La Niña phase. The precipitation deficit in response to La Niña events and its impacts on agriculture in CSA have been extensively analysed (Barrucand et al. 2007; Minetti et al. 2007; Penalba and Rivera 2016; Anderson et al. 2017). However, the ENSO cold phase does not always lead to intense droughts over the region (Sgroi et al. 2021). Other factors, such as the development of blocking conditions over the Southern Pacific Ocean (Alessandro 2008), warm Sea Surface Temperature (SST) anomalies over the tropical North Atlantic (Mo and Berbery 2011) and other regional and local factors, can contribute to the onset and intensification of drought events over this region. For example, there is a higher sensitivity of the evapotranspiration to changes in soil moisture content when the soil is dry (Ruscica et al. 2015).

Recently, the third La Niña year in a row observed since 2019 (Jones 2022) has caused a prolonged period of drought conditions over much of CSA. Central Argentina recorded 2022 as its driest year since 1960, with Argentina's core crop region experiencing its second driest year after 2008 (Ministerio de Agricultura, Ganadería y Pesca 2022). The intensification of the precipitation deficit was also evident over Uruguay during part of spring and summer, with moderate to severe drought conditions between October and December 2022 over much of the country. According to the National Institute of Meteorology from Uruguay (INUMET), the precipitation deficit ranged from -20% in the northwest to -80% in the south during spring, while December showed an increase in precipitation deficits,

with almost all the country experiencing reductions of more than -60% of total precipitation (INUMET 2022). Bolivia also experienced severe drought impacts during 2022, with almost 180 municipalities affected by precipitation shortages that threatened food security (Sistema de Información sobre Sequías para el Sur de Sudamérica 2022). As a consequence, Argentina's wheat production for 2022–2023 is projected to be nearly half of the 2021–2022 harvest, a drop from 22.4 to 12.4 million tonnes, which equals a 7-year low (Colussi et al. 2022). Similarly, its soybean production is forecast at the lowest level in over a decade; with corn exports at the lowest levels since 2017–2018 (Farm Policy News 2023). The Global Crop Monitor Report of April 2023 exhibits poor conditions for wheat and soybean over much of the Argentinean Pampas and western Uruguay (GEOGLAM 2023), with crop production losses that will significantly impact the economy of the region. More details on CSA vulnerability and exposure to droughts are given in the Supplementary Material (Section S1).

The 2019–2023 drought in CSA was triggered by several anomalous features of the atmospheric circulation at regional and hemispheric scales. Prevailing convection anomalies were evident along the Western Tropical Pacific Ocean, a region that can trigger wave trains that favour the establishment of high-pressure anomalies over CSA (Gomes et al. 2021; de Freitas et al. 2023). This circulation pattern is related to La Niña conditions (Lopes et al. 2022). In fact, considering the period from October to December (OND), high positive correlations between precipitation over the region and the Niño3.4 index are observed (Figure S1), indicating a relevant role of ENSO in the modulation of regional precipitation anomalies. Different studies suggest that the anomalous precipitation deficit in the region can also be linked to a reduced moisture transport toward the region, with reduced specific humidity values and a decrease in the northern flow from the Amazon (Gomes et al. 2021; Marengo et al. 2021). Moreover, the observed impacts of this drought have been exacerbated by the simultaneous occurrence of heat waves during November–December 2022 (Rivera et al. 2023).

Human-induced climate changes are among the factors that could enhance the occurrence of droughts due to changes in precipitation, soil moisture and temperature (Seneviratne et al. 2021). Therefore, this study focuses on identifying the possible role played by climate change in the precipitation deficits observed during the late-spring/early-summer of 2022 in CSA, using attribution methodologies previously published in peer-reviewed literature based on observational and reanalysis data and model results.

2 Data and methods

The available station data began in around 1960, with high-resolution gridded datasets being available from around 1980 onwards. Therefore, we use observed records of precipitation and temperature from more than one dataset in this study, for finding the best-fit distribution and estimating return periods, as accurately as possible. In addition to precipitation, we consider the effective precipitation during the season, obtained after subtracting the potential evapotranspiration (PET) from actual precipitation, for evaluating the effect of climate change on the amount of water actually reaching the soil. However, we limit this analysis to climate models only, due to challenges associated with observed data products for PET. These challenges are associated with the unavailability of real-time observed data, e.g. satellite-based Global Land Evaporation Amsterdam Model (GLEAM) data product is available only until December 2021 (https://www.gleam.eu/), and the large uncertainties in

the monthly anomalies from different observed data products over South America (Fig. 8 in Sörensson and Ruscica 2018).

2.1 Observational data

2.1.1 Station data

The station data over the study region was provided by the Regional Climate Center Network for Southern South America (CRC-SAS). The CRC-SAS offers climate services in support of the National Meteorological and Hydrometeorological Services and other users from Argentina, Bolivia, Brazil, Chile, Paraguay and Uruguay. From the original dataset, consisting of 454 meteorological stations with precipitation and temperature records spanning the period 1961–2022, we selected nine representative stations located over the region with higher drought severity (Fig. 1).

2.1.2 Gridded datasets

A variety of gridded datasets were analysed for the characterisation of precipitation and temperature over the study area. We use precipitation and temperature data from the European Centre for Medium-Range Weather Forecasts (ECWMF) ERA5 reanalysis (Hersbach et al. 2020), with records beginning in the year 1950. It should be noted that the variables from ERA5 are not completely based on observations, but also depend on the forecasts that are generated by atmospheric components of the Integrated Forecast System (IFS) modelling system. The Climate Prediction Center (CPC) Global Unified Gauge-Based Analysis product is provided by the National Oceanic and Atmospheric Administration (NOAA)–Physical Science Laboratory (PSL) and has daily gridded observations for precipitation and maximum and minimum temperature, available at $0.5° \times 0.5°$ resolution, for the period 1979 to present.
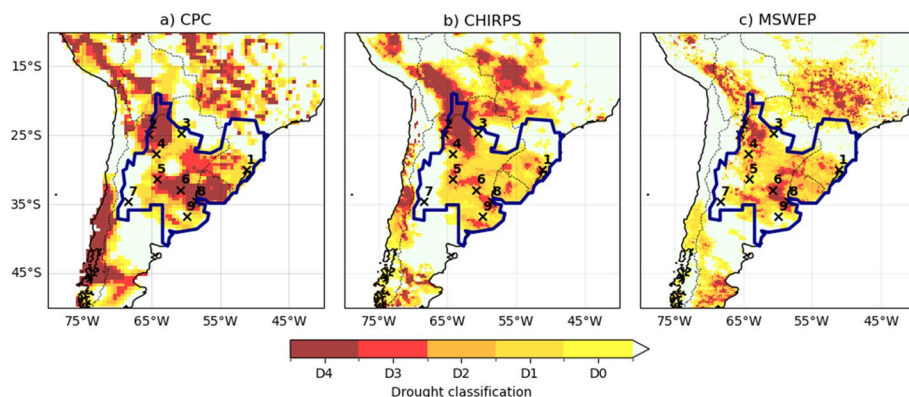

Fig. 1 Drought classifications based on the 3-month Standardised Precipitation Index (US Drought Monitor, 2023), reflecting the magnitude of the precipitation deficit from October to December 2022 relative to the 1980–2010 climatology in three gridded data products. The bold blue outline represents the study region and the crossed mark stations used in the observational analysis: 1, Porto Alegre; 2, Salta; 3, Las Lomitas; 4, Santiago del Estero; 5, Córdoba; 6, Rosario; 7, San Rafael; 8, Buenos Aires; 9, Azul

Two datasets combining satellite estimations and rain gauge information were also analysed. The Climate Hazards Group InfraRed Precipitation with Station (CHIRPS) is a quasi-global rainfall dataset, spanning 50°S–50°N (and all longitudes) and ranging from 1981 to near-present. CHIRPS incorporates CHPclim, 0.05° resolution satellite imagery and in situ station data to create gridded rainfall time series (Funk et al. 2015). The Multi-Source Weighted-Ensemble Precipitation (MSWEP) v2.8 dataset (updated from Beck et al. 2019) is fully global, available at 3-hourly intervals, and at 0.1° spatial resolution, available from 1979 to ~3 h from real time. This product combines gauge-, satellite- and reanalysis-based data for reliable precipitation estimates. Considering the data availability, we used 1981–2022 as the common period for the three gridded precipitation datasets.

As a measure of anthropogenic climate change, we use the global mean surface temperature (GMST), where GMST is taken from the National Aeronautics and Space Administration (NASA) Goddard Institute for Space Science (GISS) surface temperature analysis (GISTEMP; Hansen et al. 2010; Lenssen et al. 2019). We applied a low-pass smoothing to the GMST time series to remove the fluctuations in the global mean temperature due to ENSO, which would contaminate the global warming fingerprint with ENSO teleconnections (Philip et al. 2020).

2.2 Event definition

The expected far-reaching impact of the 2022 CSA drought on crop health and productivity is governed by the deficient rainfall at the beginning of the rainy season during October–November-December (OND), which covers most of the crop growing season in this region (Anderson et al. 2018). Therefore, for arriving at an event definition, we use the Standardised Precipitation Index (SPI, McKee et al. 1993) for an accumulation period of 3 months (SPI-3). This index is typically used in agricultural drought assessment as it captures the response of rainfall on soil moisture conditions (Spennemann et al. 2015). Figure 1 shows the SPI-3-drought classification map based on the CPC, CHIRPS and MSWEP datasets for the 2022 OND season, for a large area encompassing the affected region (5–60°S, 30–90°W). These maps are prepared based on the US Drought Monitor classifications (D0-abnormally dry, D1-moderate, D2-severe, D3-extreme and D4-exceptional; https://droughtmonitor.unl.edu/About/AbouttheData/DroughtClassification.aspx). Table S1 shows the classification thresholds and the respective rainfall thresholds for each dataset used.

We select a spatially and climatologically homogeneous area where the drought was moderate or substantial during the 3-month period from October to December and prone to agricultural loss, as the study region (blue highlighted area in Fig. 2). This region, which corresponds to CSA, includes southern Brazil (Paraná, Rio Grande do Sul and Santa Catarina provinces), central and northern Argentina (all states to the north of Buenos Aires), Uruguay and the two southernmost provinces of Bolivia (Tarija and Chuquisaca). The areas with elevation higher than 1500 m a.s.l., located in the western portion of Argentina in the adjacencies of the Andes, were excluded from the study region. It may be noted that the selected region encompasses the key agricultural states of Argentina (Llano and Vargas 2016) and also states in Brazil where vast amounts of soy, rice and wheat are produced (Mattiuzi et al. 2022). The region experienced severe impacts due to the ongoing 2019–2023 drought conditions (Naumann et al. 2023).

Based on the analysis above, for the rest of the study, we define the event by the average precipitation during OND months and area-averaged over the study region shown in
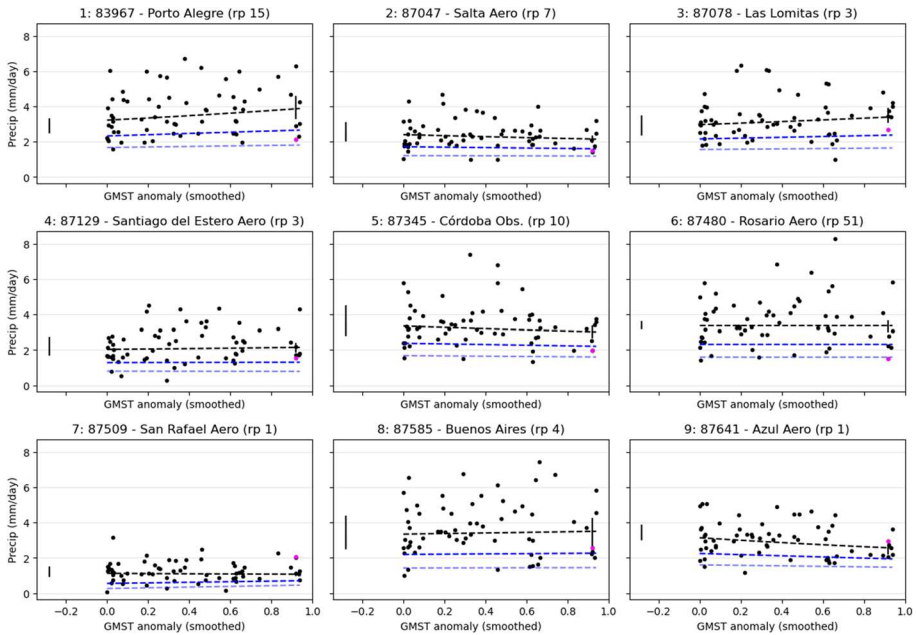
Fig. 2 Fitted trends in log-transformed OND precipitation at the nine selected stations with respect to smoothed GMST. Results are transformed back to native rainfall units of mm/day. The dots represent observed OND values, with the 2022 event highlighted in magenta. The dotted black line shows the centre of the distribution, and the blue lines represent the estimated 6-year and 40-year return levels over time. The vertical lines indicate the uncertainty about the location of the centre of the distribution in the current climate and in a 1.2 °C cooler climate. Return periods (in years) of the 2022 event are given in brackets

Fig. 1. Given that OND 2022 was also anomalously warm and characterised by multiple heat waves (Rivera et al. 2023), we additionally evaluate the effect of temperature, in particular, whether and to what extent climate change may have influenced the evapotranspiration rates, thereby exacerbating the drought.

2.3 Model and experiment descriptions

We consider multiple climate model ensembles from climate modelling experiments that use very different framings (Philip et al. 2020): SST-driven global circulation high-resolution models (HighRes), coupled global circulation models (GCMs) and regional climate models (RCMs).

2.3.1 CORDEX

The COordinated Regional climate Downscalling EXperiment (CORDEX; Gutowski et al. 2016; Giorgi et al. 2021) considers simulations resulting from pairings of GCMs and RCMs. These simulations are composed of historical simulations up to 2005 and extended to the year 2100 using the RCP8.5 scenario (Riahi et al. 2011). For the region considered in this study, we used a multi-model ensemble composed of 12 model runs available at 0.44° resolution (SAM-44 domain) and six model runs at 0.22° resolution (SAM-22 domain).

2.3.2 FLOR and AM2.5C360

The FLOR (Vecchi et al. 2014) and AM2.5C360 (Yang et al. 2021; Chan et al. 2021) models are developed at the Geophysical Fluid Dynamics Laboratory (GFDL). The FLOR model is an atmosphere–ocean coupled GCM with a resolution of 50 km for land and atmosphere and 1° for ocean and ice. Ten ensemble simulations from FLOR are analysed, which cover the period 1860–2100 and include both the historical and RCP4.5 experiments driven by transient radiative forcings from CMIP5 (Taylor et al. 2012). The AM2.5C360 is an atmospheric GCM based on the FLOR model (Delworth et al. 2012; Vecchi et al. 2014) with a horizontal resolution of 25 km. Three ensemble simulations of the Atmospheric Model Intercomparison Project (AMIP) experiment (1871–2050) are analysed. These simulations are initialised from three different pre-industrial conditions but forced by the same SSTs from the Hadley Centre Global Sea Ice and Sea Surface Temperature (HadISST1) (Rayner et al. 2003) after groupwise adjustments (Chan et al. 2021) over 1871–2020. SSTs between 2021 and 2050 use the FLOR RCP4.5 experiment 10-ensemble mean values after bias correction. Radiative forcings use historical values over 1871–2014 and RCP4.5 values after that.

2.3.3 CMIP6

The Coupled Model Intercomparison Project Phase Six (CMIP6) consists of simulations from 27 participating models with varying resolutions (Eyring et al. 2016). For all simulations, the period 1850–2015 is based on historical simulations, while the SSP5-8.5 scenario (Riahi et al. 2017) is used for the remainder of the twenty-first century.

2.3.4 HighResMIP

The HighRes Model Intercomparison Project (HighResMIP) SST-forced model ensemble (Haarsma et al. 2016) includes simulations for the period 1950–2050. The SST and sea ice forcings for the period 1950–2014 are obtained from the 0.25°×0.25° HadISST1 dataset that has undergone area-weighted regridding to match the climate model resolution. For the 'future' time period (2015–2050), SST/sea ice data are derived from RCP8.5 (CMIP5) data and combined with greenhouse gas forcings from SSP5-8.5 (CMIP6) simulations (see Section 3.3 of Haarsma et al. (2016) for further details).

2.3.5 UKCP18 land-GCM

This is a 15-member perturbed physics ensemble developed by the UK Met Office (Lowe et al. 2018). The ensemble members are derived from HadGEM3-GC3.05, a high-resolution coupled ocean–atmosphere model with a horizontal grid spacing of approximately 60 km at mid-latitudes, which includes an explicit representation of atmospheric aerosols. Historical simulations span the 1900–2005 period while projections correspond to the RCP2.6 and RCP8.5 scenarios for the period 2006–2099 (Pope et al. 2022).

2.4 Statistical methods

In this study, we analyse time series for the CSA region (Fig. 2) of precipitation, temperature and effective precipitation (PET—precipitation) for the OND season, where long

records of observed data are available. Methods for observational and model analysis and for model evaluation and synthesis are used according to the World Weather Attribution Protocol (https://www.worldweatherattribution.org), described by Philip et al. (2020) and supporting details provided by van Oldenborgh et al. (2021) and Ciavarella et al. (2021).

The analysis steps are detailed in the following sections and include (i) trend calculation from observations (Section 3); (ii) model evaluation (Section S5 in the Supplementary Material); (iii) multi-method multi-model attribution (Section 4.1); and (iv) synthesis of the attribution statement (Section 4.2). The method underlying these steps is to statistically model the event under study. We use a nonstationary Generalised Extreme Value (GEV) distribution in which the location parameter shifts with GMST, while the dispersion (the ratio of the standard deviation to the mean) remains fixed. We calculate the return periods, probability ratio (PR; the factor change in the event's probability) and change in intensity of the event under study, in order to compare the climate of the present (2022) and the past (pre-industrial; 1850–1900) periods, defined by the GMST values of both periods, based on the Global Warming Index (GWI; https://www.globalwarmingindex.org). The difference in the GMST level between the present and past periods based on this GWI is 1.2 °C.

To statistically model the precipitation associated with the event under study, we use a Gaussian distribution that scales with GMST for log-transformed precipitation. For modelling the temperature and effective precipitation, we use a Gaussian distribution that shifts with GMST. Next, results from observations and models that pass the evaluation tests are synthesised into a single attribution statement.

3 Observational analysis: return period and trend

3.1 Analysis of point station data

Figure 2 shows trends in average OND rainfall for the nine selected weather stations situated across the CSA domain (Fig. 2). The trends are fitted using a nonstationary GEV with GMST as a covariate, to identify trends driven by global warming. The method is detailed in Philip et al. (2020). The different locations represented by the nine stations show different trends, none of which are particularly strong. Rainfall at (1) Porto Alegre and (3) Las Lomitas is found to increase with GMST, whereas at (2) Salta, (5) Córdoba and (9) Azul, it is found to decrease. No trend is discernible at the remaining stations examined. Figure 3 shows the same data but represented as a return period plot to inspect the tails of the distribution and estimate the return time of the event in 2022 in today's and a 1.2 °C cooler climate. The return period of the 2022 rainfall event in the current climate ranges from 1 to 51 years at these stations, rendering the 2022 meteorological drought a relatively common event with return times on the order of 10 years in most places.

3.2 Analysis of gridded data

Figure 4 shows the trend-fitting results for the OND precipitation, area-averaged over CSA, based on three gridded datasets: CHIRPS (Fig. 4a), CPC (Fig. 4b) and MSWEP (Fig. 4c). The left panels show the log-transformed variable as a function of the GMST anomaly, while the right panels show the Gaussian distribution-based return period curves for the log-transformed variable in the present 2022 climate (red lines) and the past climate when the global mean temperature was 1.2 °C cooler (blue lines) for the respective datasets. Due
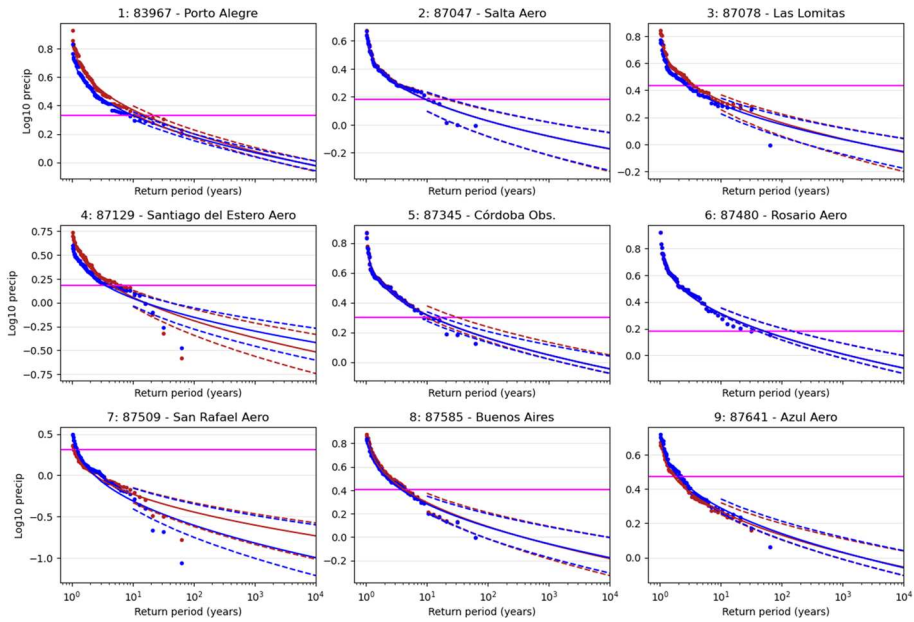
Fig. 3 Gaussian-based return periods of log-transformed rainfall for the 2022 climate (red lines) and the 1.2 °C cooler climate (blue lines) with 95% CI, at the nine selected stations. The observed event value is shown by the horizontal magenta line

to the short data length (42–44 years) and the high rainfall variability over the region (Garreaud et al. 2009; Blázquez and Solman 2017), two of the datasets (CPC and MSWEP) show a decreasing trend in rainfall whereas it is not discernible for CHIRPS. The best-estimated return period of the 2022 event is 20, 30 and 14 years, for the respective datasets (right panels of Fig. 4). Since none of the datasets is long enough to estimate the return period with enough confidence, we round these to an average of 1-in-20 years for the attribution analysis. The drought is five times and three times more likely in the 2022 climate, from the CPC and MSWEP datasets, respectively. However, these are not statistically significant, with uncertainty bands of [0.4, 135] and [0.3, 52], respectively. The respective intensity changes of a best estimate of -15% and -13%, respectively, imply that the 2022 drought is made drier by these amounts due to climate change, but again, are not statistically significant.

Figure S2 shows similar plots for the OND average temperature, area-averaged over the study region, based on two gridded data products: CPC and ERA5. From both datasets, the 2022 temperature is approximately a 1-in-2-year event in the current climate (right panels in Figure S2).
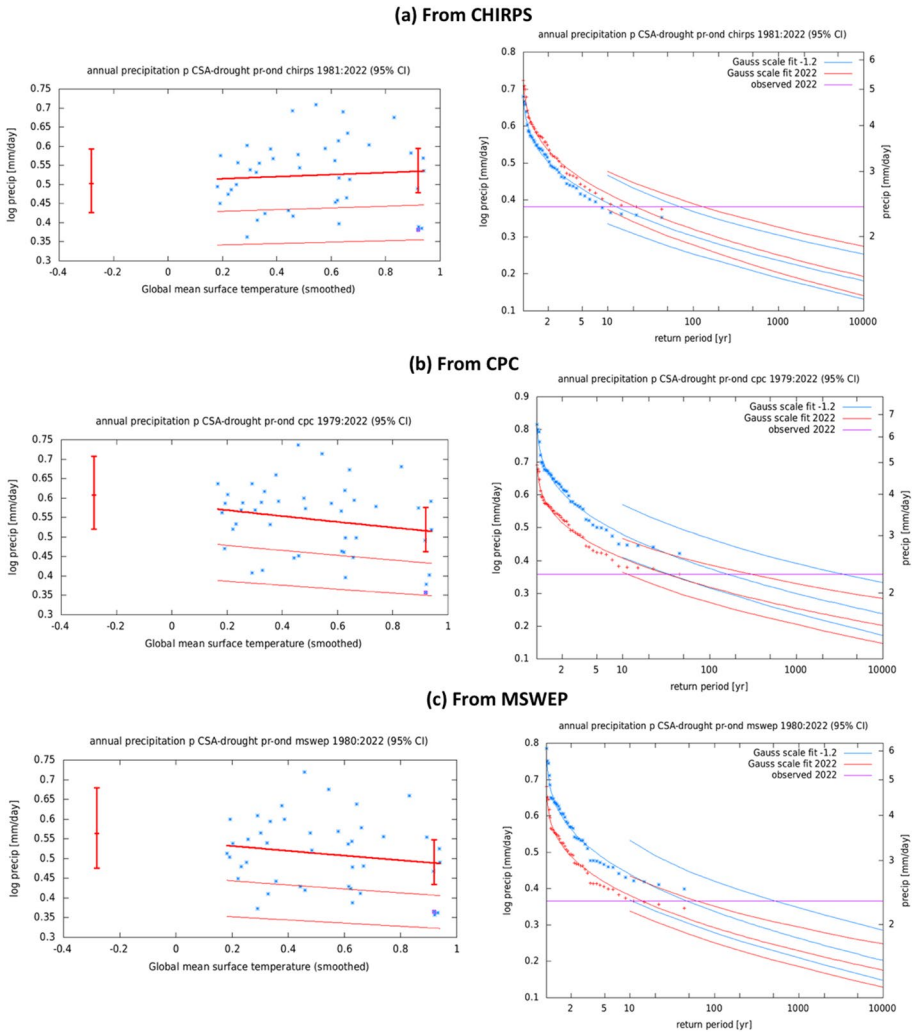
Fig. 4 (**a**, left) Response of OND rainfall (log-transformed), averaged over the CSA region to change in global mean temperature, based on the CHIRPS dataset (left). The thick red line denotes the time-varying mean, and the thin red lines show 1 standard deviation (s.d) and 2 s.d below. The vertical red lines show the 95% confidence interval (CI) for the location parameter, for the current 2022 climate and the hypothetical 1.2 °C cooler climate. The 2022 observation is highlighted with the magenta box. (**a**, right) Gaussian-based return periods of log-transformed rainfall for the 2022 climate (red lines) and the 1.2 °C cooler climate (blue lines) with 95% CI, based on the CHIRPS dataset. (**b**, left and right) same as (**a**), based on the CPC dataset. (**c**, left and right) same as (**a**), based on the MSWEP dataset

4 Model evaluation, multi-method multi-model attribution and hazard synthesis

4.1 Model evaluation and multi-method multi-model attribution

Before conducting an attribution analysis, we perform an evaluation of the models described in Section 2.3 regarding their representation of precipitation and surface

temperature over CSA. Due to limitations in observed evapotranspiration products (discussed in Section 2), we do not validate the models for the effective precipitation. Instead, we choose those models that pass the evaluation for both precipitation and temperature for attribution analysis of this variable. For model setup, we also use models that only just pass the evaluation tests if we only have five models or less for that framing that perform well. Tables S2 and S3 show the model evaluation results. The climate models are evaluated against the observations in their ability to capture the seasonal cycle, the spatial pattern of the climatology and the parameters of the fitted Gaussian/Generalised Extreme Value models. The models are labelled as 'good', 'reasonable' or 'bad', following the criteria defined in Ciavarella et al. (2021), based on their performances in terms of the three criteria discussed above. We also analysed the PRs and change in event intensity (ΔI) in the climate models for precipitation (Table S4), temperature (Table S5) and effective precipitation (Table S6) in the CSA region during the 2022 OND season. These tables show the model-based results for the models that are labelled 'reasonable' or 'good' (Tables S2 and S3). In general, the considered models have a reasonable-to-good representation of the climatological OND spatial patterns and the annual cycle for both precipitation and temperature in CSA (Tables S2 and S3, and Figures S3 to S22); however, many of them do not show a good representation of the PR and change in event intensity (Tables S2 and S3). A more detailed model evaluation is presented in the Supplementary Material (Section S5).

4.2 Hazard synthesis

In order to identify whether anthropogenic climate change did causally contribute to the low rainfall as well as the low water availability for the considered drought event, we calculate PR and the change in intensity (ΔI) using observations and climate models for the region and time period defined above in rainfall as well as effective precipitation. Models which do not pass the evaluation tests described above are excluded from the analysis. The aim is to synthesise results from models that pass the evaluation along with the observations-based products, to give an overarching attribution statement. Figures 5 and 7 show the changes in probability and intensity for observations (blue) and models (red) for precipitation and temperature, respectively. For effective precipitation (Fig. 6), we only show models (red). Figures 5 and 7 show the results of combining observations and models into a synthesised assessment, following Philip et al. (2020). See also Li and Otto (2022) for more details.

Observation-based products and models are combined into a single result in two ways. Firstly, we neglect common model uncertainties beyond the intermodel spread that is depicted by the model average, and compute the weighted average of models and observations. As model uncertainty can be larger than the intermodel spread, due to common model uncertainties, we also compute the more conservative estimate of an unweighted, direct average of observations and models, contributing 50% each.

In the results shown here for precipitation (Fig. 5), the models show a wetting trend that is not significant in many individual models, but only when models are combined (dark red bar). The observations do not show a significant trend, or change in intensity and probability. When combining the three data products, there is a small and not significant increase in the probability and intensity of drought.

When looking at effective precipitation (Fig. 6), for which we have no observations, we see mostly insignificant changes in both directions, depending on the model, but no
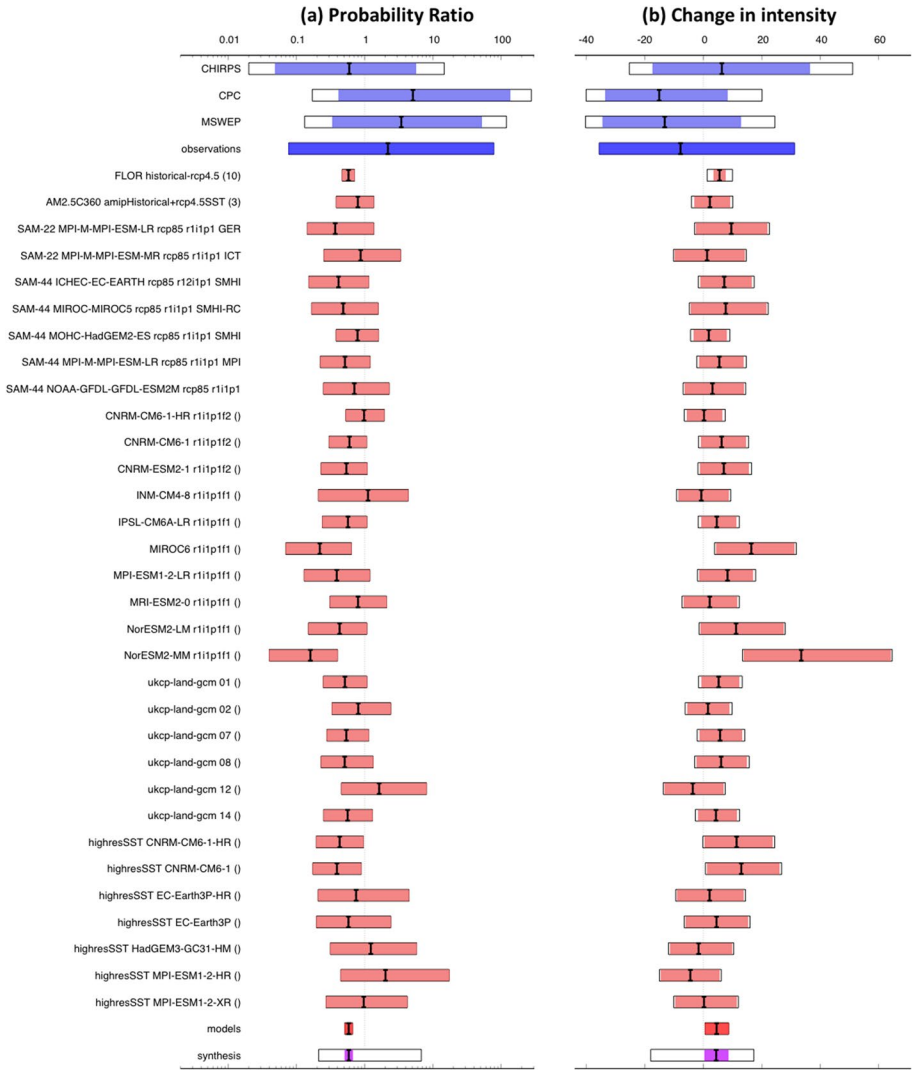
Fig. 5 Synthesis of (a) probability ratios and (b) intensity changes when comparing the return period and magnitudes of the 2022 OND precipitation in the current climate and a 1.2 °C cooler climate. White boxes around the light blue bars show a representation error (in quadrature) to the observations, to account for the difference between observations-based datasets that cannot be explained by natural variability. The dark blue bar shows the average over the observation-based products. White boxes around the light red bars show a term to account for intermodel spread that is added (in quadrature) to the natural variability of the models. The dark red bar shows the model average, consisting of a weighted mean using the (uncorrelated) uncertainties due to natural variability. The magenta bar shows the weighted average of models and observations. The white box around the magenta bar shows an unweighted, direct average of observations and models

trend is emerging. Thus, while there is a wetting in the models when looking at precipitation alone, this is not present when looking at effective precipitation. This could mean that while anthropogenic climate change does lead to an increase in rainfall and thus a decrease
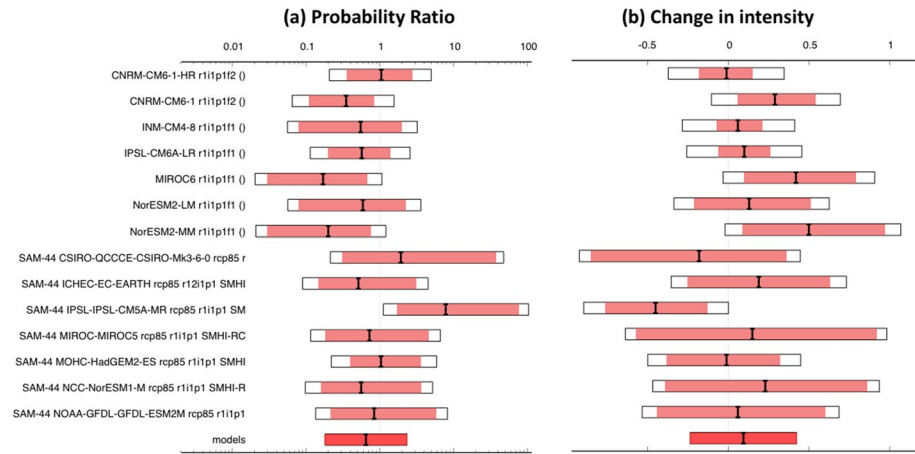
Fig. 6 As in Fig. 5 but for effective precipitation. No observational data is available for this variable

in drought, this is counteracted by the increase in temperature, and thus how much water actually would reach the ground, as indicated by the lack of any trend in effective precipitation. This is corroborated when looking at the same event definition but instead of in a 1.2 °C colder climate, in a 0.8 °C warmer climate (Figures S23 to S25). There, we observe a further wetting in the precipitation (dark red bars in Figure S23) but not when looking at effective precipitation (Figure S24).

When looking at the change in temperature for the same region and season, we identify a clear increase in the likelihood of such a temperature event to occur by a factor of 20 (2.6–180) (Fig. 7, left-hand side) and an increase in intensity by approximately 1 °C.

Combining all these lines of evidence from the synthesis results of the past climate, results from future projections and the differences in effective precipitation, precipitation and temperature, we conclude that the drought itself, represented as low rainfall, cannot be attributed to anthropogenic climate change. Nevertheless, the anthropogenic trend in temperature increases the impacts of drought (Vicente-Serrano et al. 2014; Seneviratne et al. 2021), for example favouring increased rates of soil moisture depletion (Forstner et al. 2023) and controlling biogeochemical processes such as water eutrophication (Gervasio et al. 2023).

5 Summary and discussion

Central South America (CSA) has suffered from drought for the last 3 years (2019–2023), corresponding to three consecutive La Niña events. Central Argentina recorded 2022 as its driest year since 1960, with Argentina's core crop region experiencing its second driest year after 2008. There is a high correlation between the rainfall deficit in the region during October–November-December (OND) and the Niño3.4 index, indicating that the rainfall deficit is partly driven by La Niña, as observed in previous droughts.

In order to identify whether human-induced climate change was also a driver of the rainfall deficit observed during the OND 2022 in CSA, we analysed rainfall over the most impacted region and in nine representative stations. For the region as a whole (Fig. 1),

Fig. 7 As in Fig. 5 but for temperature   ►

the event has a return period of 20 years, meaning it has a 5% chance of occurrence in any given year. At individual stations, it is a less common event, with return times up to 50 years. In the observations over the whole region, we observed a trend of reduced rainfall over the last 40 years, although we cannot be confident that this trend is beyond what is expected from natural variability in the region (Fig. 2).

To identify if the observed reduced rainfall is a real trend beyond natural variability that can be attributed to climate change, we looked at once in 20-year low rainfall events over the same region in climate models finding that the models show that low rainfall events decrease (i.e. they become wetter, the opposite of the trend observed in most weather records), although this trend is again not significant and is compatible with natural variability (Fig. 5). Therefore, we cannot attribute the low rainfall to climate change.

This does not rule out that climate change affected other aspects of the drought. Thus, to investigate whether the high temperatures, which are in part attributable to climate change, led to a deficit in water availability, calculated as potential evapotranspiration subtracted from the rainfall, we repeated the analysis for this indicator. The results show that, in climate models, the increase in temperature (Fig. 7) does partly compensate for the increase in rainfall but only to offset the wetting, and does not lead to a significant climate change signal in effective precipitation (Fig. 6). However, higher temperatures in the region, which have been attributed to climate change (Rivera et al. 2023), decreased water availability in the models in late 2022, indicating that climate change probably reduced water availability over this period also in the observations, increasing agricultural drought, although this study did not quantify this effect. This means that even though the reduced rainfall is within the natural variability, the consequences of drought are becoming more severe due to the strong increase in extreme heat. In fact, the occurrence of concurrent droughts and heat waves has increased in frequency over the last century at the global scale due to human influence and this trend will continue with increasing global warming levels (Seneviratne et al. 2021). This has been shown to exacerbate water-related impacts, for instance, heat stress, tree mortality, food prices and water insecurity, among others (e.g. Singh et al. 2018; Anderson et al. 2019; Seneviratne et al. 2021; Caretta et al. 2022).

Another aspect possibly influencing the current drought in CSA is the alteration of atmospheric moisture transport patterns in association with land use changes. Different studies have shown that droughts can be triggered or exacerbated by changes in atmospheric moisture transport (Feng et al. 2011; Drumond et al. 2016, 2017, 2019, 2021; Sorí et al. 2017; Salah et al. 2018; Stojanovic et al. 2018a, 2018b; Herrera-Estrada et al. 2019; Miralles et al. 2019). The main moisture sources for CSA, especially the La Plata Basin (LPB), are the terrestrial sources, including local recycling (with a contribution of about 23% of the mean annual precipitation in the region) and the southern Amazon (contributing about 20%) (Martinez and Dominguez 2014; Zemp et al. 2014). In particular, the moisture transported from the southern Amazon during the dry season is more efficiently converted to precipitation over LPB than that originated in LPB itself (i.e. recycling) (Martinez and Dominguez 2014). Drumond et al. (2019) analysed the links between anomalous moisture transport and droughts in CSA, finding that for instance, the 2008–2009 drought was associated with reductions of moisture contributions from terrestrial sources, including the southern Amazon. This suggests that the reduction of atmospheric moisture transported from the southern Amazon could be an important contributor to the precipitation deficits during drought events in LPB.

(a) Probability Ratio   (b) Change in intensity
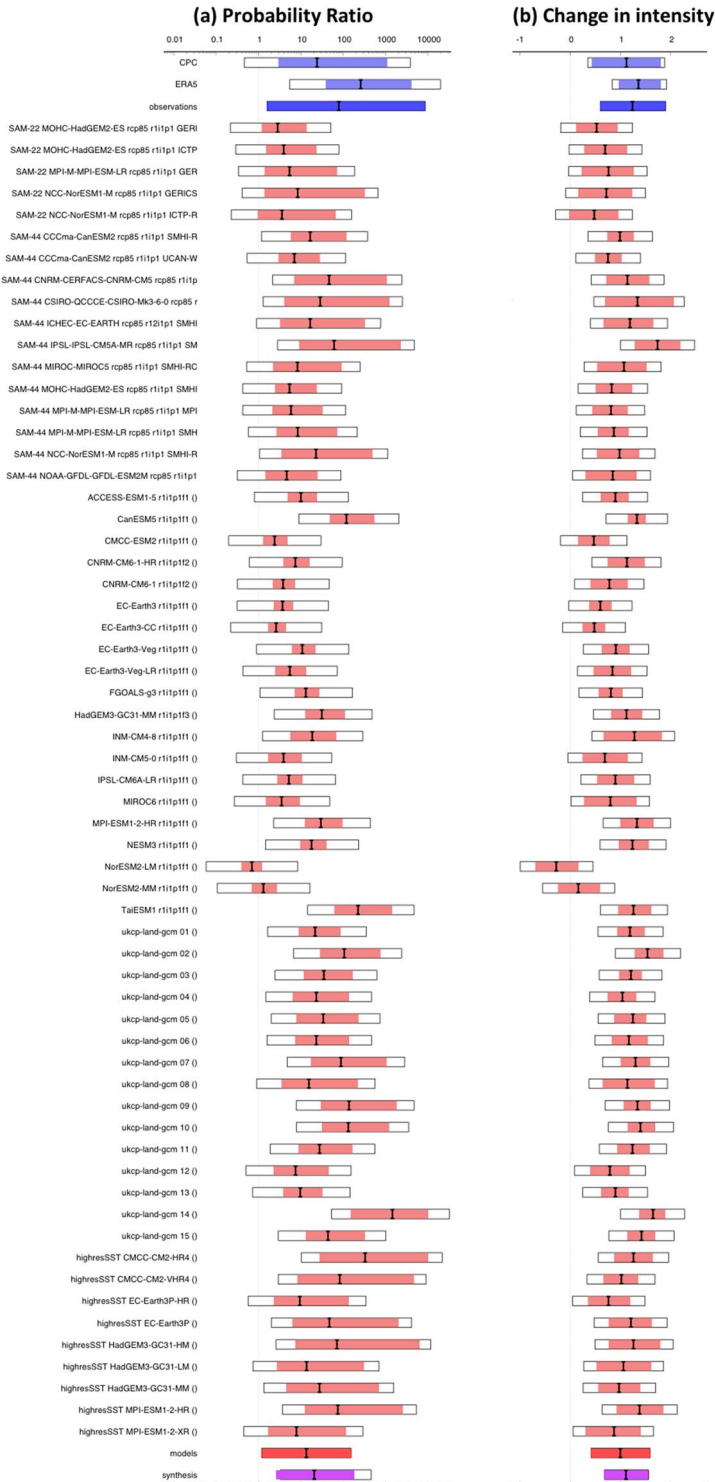
Deforestation of the Amazon forests, particularly in the southern Amazon, is a driver of reductions of not only local atmospheric moisture recycling but also atmospheric moisture transport toward other regions (e.g. Zemp et al. 2014; Molina et al. 2019; Ruiz-Vásquez et al. 2020). For instance, Ruiz-Vásquez et al. (2020) show that scenarios with deforested areas of about 28–38% in the Amazon exhibit reduced contributions of water vapour toward northern South America of about 40–43%. Based on the analysis of climatological cascading moisture recycling, Zemp et al. (2014) discuss that the land use change in the Amazon might have a stronger impact on LPB rainfall than previously considered. This suggests that Amazon deforestation could play a role in precipitation deficits over LPB due to reductions of the atmospheric moisture that originates in the Amazon and is transported by the winds toward LPB. This is particularly important in the case of the 2022–2023 drought in CSA, given the fact that the Brazilian Amazon deforestation rate in 2020 was the greatest of the last decade (Silva Junior et al. 2021). Whether the ongoing drought in CSA is partly driven by Amazon deforestation needs to be addressed.

The case of the OND 2022 rainfall deficit and the ongoing drought in CSA is a clear example of the interplay between climate variability and human-induced climate change. In particular, the strong interannual variability imposed by the El Niño-Southern Oscillation over CSA, especially the precipitation reductions detected during La Niña, is one of the main drivers of the current drought in CSA, as also identified in previous droughts. This rainfall deficit and the subsequent drought have been amplified by the increasing temperatures and concurrent heat waves occurring over the region during OND 2022. This shows the importance of considering not only those aspects associated with climate change but also climate variability in order to understand and attribute particular events or trends at the regional level. The most recent assessment report of the Intergovernmental Panel on Climate Change discusses this in depth, showing that various mechanisms operating at different time scales can modify the amplitude of the regional-scale response of temperature, and both the amplitude and sign of the response of precipitation, to human-induced climate change (Doblas-Reyes et al. 2021).

Declarations

Ethics approval and consent to participate Not applicable.

Consent for publication All authors consent to the publication of this manuscript.

Competing interests The authors declare no competing interests.

References

Alessandro AP (2008) Anomalías de circulación atmosférica en 500 y 1000 hpa asociada a la sequía producida en la Argentina durante enero de 2003 a marzo de 2004. Rev Bras Meteorol 23(1):12–29. https://doi.org/10.1590/S0102-77862008000100002

Anderson W, Seager R, Baethgen W, Cane M (2017) Crop production variability in North and South America forced by life-cycles of the El Niño Southern Oscillation. Agric for Meteorol 239:151–165. https://doi.org/10.1016/j.agrformet.2017.03.008

Anderson W, Seager R, Baethgen W, Cane M (2018) Trans-Pacific ENSO teleconnections pose a correlated risk to agriculture. Agric for Meteorol 262:298–309. https://doi.org/10.1016/j.agrformet.2018.07.023

Anderson WB, Seager R, Baethgen W, Cane M, You L (2019) Synchronous crop failures and climate-forced production variability. Sci Adv 5(7):eaaw1976. https://doi.org/10.1126/sciadv.aaw1976

Barrucand M, Vargas W, Rusticucci M (2007) Dry conditions over Argentina and the related monthly circulation patterns. Meteorol Atmos Phys 98:99–114. https://doi.org/10.1007/s00703-006-0232-5

Beck HE, Wood EF, Pan M, Fisher CK, Miralles DG, van Dijk AIJM, McVicar TR, Adler RF (2019) MSWEP V2 global 3-hourly 0.1° precipitation: methodology and quantitative assessment. Bull Am Meteorol Soc 100(3):473–500. https://doi.org/10.1175/BAMS-D-17-0138.1

Bert F, de Estrada M, Naumann G, Negri R, Podestá G, Skansi MM, Spennemann P, Quesada M (2021) The 2017–18 drought in the Argentine Pampas: impacts on agriculture. Special Report on Drought 2021. United Nations Office for Disaster Risk Reduction, p 24. https://www.undrr.org/publication/2017-18-drought-argentine-pampas-impacts-agriculture-0

Blázquez J, Solman SA (2017) Interannual variability of the frontal activity in the Southern Hemisphere: relationship with atmospheric circulation and precipitation over southern South America. Clim Dyn 48:2569–2579. https://doi.org/10.1007/s00382-016-3223-3

Caretta MA, Mukherji A, Arfanuzzaman M, Betts RA, Gelfan A, Hirabayashi Y, Lissner TK, Liu J, Lopez Gunn E, Morgan R, Mwanga S, Supratid S (2022) Water. In: Climate change 2022: impacts, adaptation and vulnerability. Contribution of Working Group II to the Sixth Assessment Report of the Intergovernmental Panel on Climate Change [H.-O. Pörtner, D.C. Roberts, M. Tignor, E.S. Poloczanska, K. Mintenbeck, A. Alegría, M. Craig, S. Langsdorf, S. Löschke, V. Möller, A. Okem, B. Rama (eds.)]. Cambridge University Press, Cambridge, UK and New York, NY, USA, pp 551–712. https://doi.org/10.1017/9781009325844.006

Castellanos, E, Lemos MF, Astigarraga L, Chacón N et al (2022) Central and South America. In: Climate change 2022: impacts, adaptation and vulnerability. Contribution of Working Group II to the Sixth Assessment Report of the Intergovernmental Panel on Climate Change [H.-O. Pörtner, D.C. Roberts, M. Tignor, E.S. Poloczanska, K. Mintenbeck, A. Alegría, M. Craig, S. Langsdorf, S. Löschke, V. Möller, A. Okem, B. Rama (eds.)]. Cambridge University Press, Cambridge, UK and New York, NY, USA, pp 1689–1816. https://doi.org/10.1017/9781009325844.014

Chan D, Vecchi GA, Yang W, Huybers P (2021) Improved simulation of 19th- and 20th-century North Atlantic hurricane frequency after correcting historical sea surface temperatures. Sci Adv 7:eabg6931. https://doi.org/10.1126/sciadv.abg6931

Ciavarella A, Cotterill D, Stott P, Kew S, Philip S, van Oldenborgh GJ et al (2021) Prolonged Siberian heat of 2020 almost impossible without human influence. Clim Change 166(1):9. https://doi.org/10.1007/s10584-021-03052-w

Colussi J, Cabrini S, Schnitkey G, Paulson N (2022) Wheat production plunges in Argentina, on record pace in Brazil. Farmdoc Daily (12):189. Department of Agricultural and Consumer Economics, University of Illinois at Urbana-Champaign

Cruz G, Baethgen W, Bartaburu D, Bidegain M, Giménez A, Methol M, Morales H, Picasso V, Podestá G, Taddei R, Terra R, Tiscornia G, Vinocur M (2018) Thirty years of multilevel processes for adaptation

of livestock production to droughts in Uruguay. Weather Clim Soc 10(1):59–74. https://doi.org/10.1175/WCAS-D-16-0133.1

de Freitas AA, Reboita MS, Carvalho VSB, Drumond A, Ferraz SET, da Silva BC, da Rocha RP (2023) Atmospheric and oceanic patterns associated with extreme drought events over the Paraná hydrographic region, Brazil. Climate 11(1):12. https://doi.org/10.3390/cli11010012

Delworth TL, Rosati A, Anderson W, Adcroft AJ, Balaji V, Benson R, Dixon K, Griffies SM, Lee H, Pacanowski RC, Vecchi GA, Wittenberg AT, Zeng F, Zhang R (2012) Simulated climate and climate change in the GFDL CM2.5 high-resolution coupled climate model. J Clim 25(8):2755–2781. https://doi.org/10.1175/JCLI-D-11-00316.1

Doblas-Reyes FJ, Sörensson AA, Almazroui M et al (2021) Linking global to regional climate change. In Climate change 2021: the physical science basis. Contribution of Working Group I to the Sixth Assessment Report of the Intergovernmental Panel on Climate Change [Masson-Delmotte, V., P. Zhai, A. Pirani, S.L. Connors, C. Péan, S. Berger, N. Caud, Y. Chen, L. Goldfarb, M.I. Gomis, M. Huang, K. Leitzell, E. Lonnoy, J.B.R. Matthews, T.K. Maycock, T. Waterfield, O. Yelekçi, R. Yu, and B. Zhou (eds.)]. Cambridge University Press, Cambridge, United Kingdom and New York, NY, USA, pp 1363–1512. https://doi.org/10.1017/9781009157896.012

Drumond A, Nieto R, Gimeno L (2016) A Lagrangian approach for investigating anomalies in the moisture transport during drought episodes. Cuad Investig Geogr 42(1):113–125. https://doi.org/10.18172/cig.2925

Drumond A, Gimeno L, Nieto R, Trigo RM, Vicente-Serrano SM (2017) Drought episodes in the climatological sinks of the Mediterranean moisture source: the role of moisture transport. Global Planet Change 151:4–14. https://doi.org/10.1016/j.gloplacha.2016.12.004

Drumond A, Stojanovic M, Nieto R, Vicente-Serrano SM, Gimeno L (2019) Linking anomalous moisture transport and drought episodes in the IPCC reference regions. Bull Am Meteor Soc 100(8):1481–1498. https://doi.org/10.1175/BAMS-D-18-0111.1

Drumond A, Stojanovic M, Nieto R, Gimeno L, Liberato MLR, Pauliquevis T, Oliveira M, Ambrizzi T (2021) Dry and wet climate periods over Eastern South America: identification and characterization through the SPEI index. Atmosphere 12(2):155. https://doi.org/10.3390/atmos12020155

Eyring V, Bony S, Meehl GA, Senior CA, Stevens B, Stouffer RJ, Taylor KE (2016) Overview of the Coupled Model Intercomparison Project Phase 6 (CMIP6) experimental design and organization. Geosci Model Dev 9:1937–1958. https://doi.org/10.5194/gmd-9-1937-2016

Farm Policy News (2023) Argentina soybean, corn production estimates lowered, as country's key agricultural region battles ongoing drought. Available at: https://farmpolicynews.illinois.edu/2023/03/argentina-soybean-corn-production-estimates-lowered-as-countrys-key-agricultural-region-battles-ongoing-drought/, accessed 10 March 2023

Feng S, Hu Q, Oglesby RJ (2011) Influence of Atlantic sea surface temperatures on persistent drought in North America. Clim Dyn 37:569–586. https://doi.org/10.1007/s00382-010-0835-x

Forstner V, Vremec M, Herndl M, Birk S (2023) Effects of dry spells on soil moisture and yield anomalies at a montane managed grassland site: a lysimeter climate experiment. Ecohydrology 16(3):e2518. https://doi.org/10.1002/eco.2518

Funk C, Peterson P, Landsfeld M et al (2015) The climate hazards infrared precipitation with stations—a new environmental record for monitoring extremes. Sci Data 2:150066. https://doi.org/10.1038/sdata.2015.66

Garreaud RD, Vuille M, Compagnucci R, Marengo J (2009) Present-day South American climate. Palaeogeogr Palaeoclimatol Palaeoecol 281:180–195. https://doi.org/10.1016/j.palaeo.2007.10.032

GEOGLAM (2023) Global Crop Monitor No. 9 - April 2023. https://cropmonitor.org/documents/GLOBAL/reports/Global_CropMonitor_202304.pdf. Accessed 6 April 2023

Gervasio MP, Soana E, Vincenzi F, Magri M, Castaldelli G (2023) Drought-induced salinity intrusion affects nitrogen removal in a deltaic ecosystem (Po River Delta, Northern Italy). Water 15(13):2405. https://doi.org/10.3390/w15132405

Giorgi F, Coppola E, Teichmann C et al (2021) Editorial for the CORDEX-CORE Experiment I Special Issue. Clim Dyn 57:1265–1268

Gomes MS, Cavalcanti IFA, Müller G (2021) 2019/2020 drought impacts on South America and atmospheric and oceanic influences. Weather Clim Extremes 34:100404. https://doi.org/10.1016/j.wace.2021.100404

Gutowski WJ Jr, Giorgi F, Timbal B, Frigon A, Jacob D, Kang H-S, Raghavan K, Lee B, Lennard C, Nikulin G, O'Rourke E, Rixen M, Solman S, Stephenson T, Tangang F (2016) WCRP COordinated Regional Downscaling EXperiment (CORDEX): a diagnostic MIP for CMIP6. Geosci Model Dev 9:4087–4095. https://doi.org/10.5194/gmd-9-4087-2016

Haarsma RJ, Roberts MJ, Vidale PL, Senior CA, Bellucci A, Bao Q, Chang P et al (2016) High Resolution Model Intercomparison Project (HighResMIP v1.0) for CMIP6. Geosci Model Dev 9:4185–4208. https://doi.org/10.5194/gmd-9-4185-2016

Hansen J, Ruedy R, Sato M, Lo K (2010) Global surface temperature change. Rev Geophys 48:RG4004. https://doi.org/10.1029/2010RG000345

Hernández C, Methol M, Cortelezzi A (2018) Estimación de pérdidas y daños por eventos climáticos extremos en el sector agropecuario. In: Anuario OPYPA 2018. Ministerio de Ganadería y Pesca República Oriental del Uruguay, p 10. https://www.gub.uy/ministerio-ganaderia-agricultura-pesca/sites/ministerio-ganaderia-agricultura-pesca/files/documentos/publicaciones/estimacion_de_danos_y_perdidas_por_eventos_climaticos.pdf. Accessed 25 Mar 2023

Herrera-Estrada JE, Martinez JA, Dominguez F, Findell KL, Wood EF, Sheffield J (2019) Reduced moisture transport linked to drought propagation across North America. Geophys Res Lett 46:5243–5253. https://doi.org/10.1029/2019GL082475

Hersbach H, Bell B, Berrisford P, Hirahara S, Horányi A, Muñoz-Sabater J et al (2020) The ERA5 global reanalysis. Q J R Meteorol Soc 146:1999–2049. https://doi.org/10.1002/qj.3803

INUMET (2022) Boletín Trimestral No. 4 Informe de Primavera. https://www.inumet.gub.uy/sites/default/files/2022-12/informe%20estacional%20PRIMAVERA.pdf. Accessed 25 March 2023

IPCC (2021) Summary for policymakers. In: Climate change 2021: the physical science basis. Contribution of Working Group I to the Sixth Assessment Report of the Intergovernmental Panel on Climate Change [Masson-Delmotte, V., P. Zhai, A. Pirani, S.L. Connors, C. Péan, S. Berger, N. Caud, Y. Chen, L. Goldfarb, M.I. Gomis, M. Huang, K. Leitzell, E. Lonnoy, J.B.R. Matthews, T.K. Maycock, T. Waterfield, O. Yelekçi, R. Yu, and B. Zhou (eds.)]. Cambridge University Press, Cambridge, United Kingdom and New York, NY, USA, pp 3–32. https://doi.org/10.1017/9781009157896.001

Jones N (2022) Rare 'triple' La Niña climate event looks likely — what does the future hold? Nature 607:2. https://doi.org/10.1038/d41586-022-01668-1

Lenssen NJL, Schmidt GA, Hansen JE, Menne MJ, Persin A, Ruedy R, Zyss D (2019) Improvements in the GISTEMP uncertainty model. J Geophys Res: Atmos 124:6307–6326. https://doi.org/10.1029/2018JD029522

Li S, Otto F (2022) The role of human-induced climate change in heavy rainfall events such as the one associated with Typhoon Hagibis. Clim Change 172:7. https://doi.org/10.1007/s10584-022-03344-9

Llano MP, Vargas W (2016) Climate characteristics and their relationship with soybean and maize yields in Argentina, Brazil and the United States. Int J Climatol 36:1471–1483. https://doi.org/10.1002/joc.4439

Lopes AB, Andreoli RV, Souza RAF, Cerón WL, Kayano MT, Canchala T, de Moraes DS (2022) Multiyear La Niña effects on the precipitation in South America. Int J Climatol 42(16):9567–9582. https://doi.org/10.1002/joc.7847

Lowe JA, Bernie D, Bett P, Bricheno L et al (2018) UKCP18 Science Overview Report. Met Office, London

Marengo JA, Cunha AP, Cuartas LA et al (2021) Extreme drought in the Brazilian Pantanal in 2019–2020: characterization, causes, and impacts. Front Water 3:639204. https://doi.org/10.3389/frwa.2021.639204

Martinez JA, Dominguez F (2014) Sources of atmospheric moisture for the La Plata River Basin. J Clim 27(17):6737–6753. https://doi.org/10.1175/JCLI-D-14-00022.1

Mattiuzi CDP, Marques GF, Medellin-Azuara J, Dalcin AP (2022) The economic value of water in crop productions and policy implications in southern Brazil. Proc Inst Civ Eng – Water Manag 175(1):1900084. https://doi.org/10.1680/jwama.19.00084

McKee TB, Doesken NJ, Kleist J (1993) The relationship of drought frequency and duration to time scales. Eighth Conf Appl Climatol, Anaheim, California. https://www.droughtmanagement.info/literature/AMS_Relationship_Drought_Frequency_Duration_Time_Scales_1993.pdf. Accessed 25 Mar 2023

Minetti JL, Vargas WM, Vega B, Costa MC (2007) Las sequías en la pampa húmeda: impacto en la productividad del maíz. Rev Bras Meteorol 22(2):218–232. https://doi.org/10.1590/S0102-77862007000200007

Ministerio de Agricultura, Ganadería y Pesca (2022) Informe de Sequía Diciembre 2022. https://www.magyp.gob.ar/sitio/areas/d_eda/sequia/_archivos//220000_Informes%202022/221200_Informe%20Sequ%C3%ADa%20-%20Diciembre%202022.pdf. Accessed 25 Mar 2023

Miralles DG, Gentine P, Seneviratne SI, Teuling AJ (2019) Land–atmospheric feedbacks during droughts and heat waves: state of the science and current challenges. Ann NY Acad Sci 1436:19–35. https://doi.org/10.1111/nyas.13912

Mo KC, Berbery EH (2011) Drought and persistent wet spells over South America based on observations and the U.S. CLIVAR drought experiments. J Clim 24(6):1801–1820. https://doi.org/10.1175/2010JCLI3874.1

Molina RD, Salazar JF, Martínez JA, Villegas JC, Arias PA (2019) Forest-induced exponential growth of precipitation along climatological wind streamlines over the Amazon. J Geophys Res: Atmos 124:2589–2599. https://doi.org/10.1029/2018JD029534

Naumann G, Vargas WM, Barbosa P, Blauhut V, Spinoni J, Vogt JV (2019) Dynamics of socioeconomic exposure, vulnerability and impacts of recent droughts in Argentina. Geosciences 9(1):39. https://doi.org/10.3390/geosciences9010039

Naumann G, Podestá G, Marengo J et al (2023) Extreme and long-term drought in the La Plata Basin: event evolution and impact assessment until September 2022. Publ Off Eur Union Luxembourg. https://doi.org/10.2760/62557

Penalba OC, Rivera JA (2016) Precipitation response to El Niño/La Niña events in Southern South America – emphasis in regional drought occurrences. Adv Geosci 42:1–14. https://doi.org/10.5194/adgeo-42-1-2016

Philip S, Kew S, van Oldenborgh GJ, Otto F, Vautard R, van der Wiel K et al (2020) A protocol for probabilistic extreme event attribution analyses. Adv Stat Clim Meteorol Oceanogr 6:177–203. https://doi.org/10.5194/ascmo-6-177-2020

Pope JO, Brown K, Fung F et al (2022) Investigation of future climate change over the British Isles using weather patterns. Clim Dyn 58:2405–2419. https://doi.org/10.1007/s00382-021-06031-0

Rayner NA, Parker DE, Horton EB, Folland CK, Alexander LV, Rowell DP, Kent EC, Kaplan A (2003) Global analyses of sea surface temperature, sea ice, and night marine air temperature since the late nineteenth century. J Geophys Res 108(D14):4407. https://doi.org/10.1029/2002JD002670

Riahi K, Rao S, Krey V et al (2011) RCP 8.5—a scenario of comparatively high greenhouse gas emissions. Clim Chang 109:33. https://doi.org/10.1007/s10584-011-0149-y

Riahi K, van Vuuren DP, Kriegler E et al (2017) The shared socioeconomic pathways and their energy, land use, and greenhouse gas emissions implications: an overview. Glob Environ Chang 42:153–168. https://doi.org/10.1016/j.gloenvcha.2016.05.009

Rivera JA, Penalba OC (2014) Trends and spatial patterns of drought affected area in Southern South America. Climate 2(4):264–278. https://doi.org/10.3390/cli2040264

Rivera JA, Arias PA, Sörensson AA et al (2023) 2022 early-summer heatwave in Southern South America: 60 times more likely due to climate change. Clim Change 176:102. https://doi.org/10.1007/s10584-023-03576-3

Ruiz-Vásquez M, Arias PA, Martínez JA, Espinoza JC (2020) Effects of Amazon basin deforestation on regional atmospheric circulation and water vapor transport towards tropical South America. Clim Dyn 54:4169–4189. https://doi.org/10.1007/s00382-020-05223-4

Ruscica RC, Sörensson AA, Menéndez CG (2015) Pathways between soil moisture and precipitation in southeastern South America. Atmos Sci Lett 16:267–272. https://doi.org/10.1002/asl2.552

Salah Z, Nieto R, Drumond A, Gimeno L, Vicente-Serrano SM (2018) A Lagrangian analysis of the moisture budget over the Fertile Crescent during two intense drought episodes. J Hydrol 560:382–395. https://doi.org/10.1016/j.jhydrol.2018.03.021

Seneviratne SI, Zhang X, Adnan M, Badi W, Dereczynski C et al (2021) Weather and climate extreme events in a changing climate. In Climate change 2021: the physical science basis. Contribution of Working Group I to the Sixth Assessment Report of the Intergovernmental Panel on Climate Change [Masson-Delmotte, V., P. Zhai, A. Pirani, S.L. Connors, C. Péan, S. Berger, N. Caud, Y. Chen, L. Goldfarb, M.I. Gomis, M. Huang, K. Leitzell, E. Lonnoy, J.B.R. Matthews, T.K. Maycock, T. Waterfield, O. Yelekçi, R. Yu, and B. Zhou (eds.)]. Cambridge University Press, Cambridge, United Kingdom and New York, NY, USA, pp 1513–1766. https://doi.org/10.1017/9781009157896.013

Sgroi LC, Lovino MA, Berbery EH, Müller GV (2021) Characteristics of droughts in Argentina's core crop region. Hydrol Earth Syst Sci 25:2475–2490. https://doi.org/10.5194/hess-25-2475-2021

Silva Junior CHL, Pessôa ACM, Carvalho NS et al (2021) The Brazilian Amazon deforestation rate in 2020 is the greatest of the decade. Nat Ecol Evol 5:144–145. https://doi.org/10.1038/s41559-020-01368-x

Singh D, Seager R, Cook BI, Cane M, Ting M, Cook E, Davis M et al (2018) Climate and the global famine of 1876–78. J Clim 31(23):9445–9467. https://doi.org/10.1175/jcli-d-18-0159.1

Sistema de Información sobre Sequías para el Sur de Sudamérica (2022) Sequía en Bolivia. La actividad agrícola y ganadera en alerta. https://sissa.crc-sas.org/blog/2022/11/23/sequia-en-bolivia-la-actividad-agricola-y-ganadera-en-alerta/. Accessed 25 March 2023

Sörensson AA, Ruscica RC (2018) Intercomparison and uncertainty assessment of nine evapotranspiration estimates over South America. Water Resour Res 54:2891–2908. https://doi.org/10.1002/2017WR021682

Sorí R, Nieto R, Vicente-Serrano SM, Drumond A, Gimeno L (2017) A Lagrangian perspective of the hydrological cycle in the Congo River basin. Earth Syst Dynam 8:653–675. https://doi.org/10.5194/esd-8-653-2017

Spennemann PC, Rivera JA, Saulo AC, Penalba OC (2015) A comparison of GLDAS soil moisture anomalies against the Standardized Precipitation Index and Multisatellite estimations over South America. J Hydrometeorol 16:158–171. https://doi.org/10.1175/jhm-d-13-0190.1

Stojanovic M, Drumond A, Nieto R, Gimeno L (2018a) Anomalies in moisture supply during the 2003 drought event in Europe: a Lagrangian analysis. Water 10(4):467. https://doi.org/10.3390/w10040467

Stojanovic M, Drumond A, Nieto R, Gimeno L (2018b) Variations in moisture supply from the mediterranean sea during meteorological drought episodes over Central Europe. Atmosphere 9(7):278. https://doi.org/10.3390/atmos9070278

Taylor KE, Stouffer RJ, Meehl GA (2012) An overview of CMIP5 and the experiment design. Bull Am Meteorol Soc 93(4):485–498. https://doi.org/10.1175/BAMS-D-11-00094.1

Tripaldi A, Zárate MA, Forman SL, Badger T, Doyle ME, Ciccioli P (2013) Geological evidence for a drought episode in the western Pampas (Argentina, South America) during the early–mid 20th century. Holocene 23(12):1731–1746. https://doi.org/10.1177/0959683613505338

van Oldenborgh GJ, van der Wiel K, Kew S, Philip S, Otto F, Vautard R et al (2021) Pathways and pitfalls in extreme event attribution. Clim Change 166(1):13. https://doi.org/10.1007/s10584-021-03071-7

Vecchi GA, Delworth T, Gudgel R et al (2014) On the seasonal forecasting of regional tropical cyclone activity. J Clim 27(21):7994–8016. https://doi.org/10.1175/JCLI-D-14-00158.1

Vicente-Serrano S, Lopez-Moreno JI, Begueria S et al (2014) Evidence of increasing drought severity caused by temperature rise in southern Europe. Env Res Lett 9:044001. https://doi.org/10.1088/1748-9326/9/4/044001

Yang W, Hsieh T-L, Vecchi GA (2021) Hurricane annual cycle controlled by both seeds and genesis probability. PNAS 118(41):e2108397118. https://doi.org/10.1073/pnas.2108397118

Zemp DC, Schleussner C-F, Barbosa HMJ, van der Ent RJ, Donges JF, Heinke J, Sampaio G, Rammig A (2014) On the importance of cascading moisture recycling in South America. Atmos Chem Phys 14:1333–13359. https://doi.org/10.5194/acp-14-13337-2014

Authors and Affiliations

Paola A. Arias[1] [ORCID] · **Juan Antonio Rivera[2]** · **Anna A. Sörensson[3,4,5]** · **Mariam Zachariah[6]** · **Clair Barnes[6]** · **Sjoukje Philip[7]** · **Sarah Kew[7]** · **Robert Vautard[8]** · **Gerbrand Koren[9]** · **Izidine Pinto[7]** · **Maja Vahlberg[10]** · **Roop Singh[10]** · **Emmanuel Raju[11]** · **Sihan Li[12]** · **Wenchang Yang[13]** · **Gabriel A. Vecchi[13,14]** · **Friederike E. L. Otto[6]**

✉ Paola A. Arias
paola.arias@udea.edu.co

[1] Grupo de Ingeniería y Gestión Ambiental (GIGA), Escuela Ambiental, Facultad de Ingeniería, Universidad de Antioquia, Medellin, Colombia

[2] Glaciología y Ciencias Ambientales (IANIGLA), Instituto Argentino de Nivología, CCT CONICET, Mendoza, Argentina

[3] Facultad de Ciencias Exactas y Naturales, Universidad de Buenos Aires, Buenos Aires, Argentina

[4] CONICET–Universidad de Buenos Aires, Centro de Investigaciones del Mar y La Atmósfera, Buenos Aires, Argentina

[5] CNRS–IRD–CONICET–UBA, Instituto Franco-Argentino Para El Estudio del Clima y Sus Impactos (IRL 3351 IFAECI), Buenos Aires, Argentina

[6] Grantham Institute, Imperial College London, London, UK

[7] Royal Netherlands Meteorological Institute (KNMI), De Bilt, the Netherlands

[8] Institut Pierre-Simon Laplace, Paris, France

[9] Copernicus Institute of Sustainable Development, Utrecht University, Utrecht, the Netherlands

[10] Red Cross Red Crescent Climate Centre, The Hague, the Netherlands

[11] Department of Public Health, Global Health Section & Copenhagen Centre for Disaster Research, Copenhagen, Denmark

[12] Department of Geography, University of Sheffield, Sheffield, UK

[13] Department of Geosciences, Princeton University, Princeton, NJ 08544, USA

[14] High Meadows Environmental Institute, Princeton University, Princeton, NJ 08544, USA